land

MDPI

Article

Landscape-Scale Long-Term Drought Prevalence Mapping for Small Municipalities Adaptation, the Czech Republic Case Study

Ludmila Floková [1,2] and Tomáš Mikita [1,*]

[1] Department of Forest Management and Applied Geoinformatics, Faculty of Forestry and Wood Technology, Mendel University in Brno, 613 00 Brno, Czech Republic; ludmila.flokova@mendelu.cz
[2] Institute of Environmental Science and Natural Resources, Faculty of Regional Development and International Studies, Mendel University in Brno, 613 00 Brno, Czech Republic
* Correspondence: tomas.mikita@mendelu.cz

Abstract: Drought is a phenomenon that is strengthening with the progress of climate change. Many fields of human activities such as agriculture, forestry, ecology, economy, water supply, or energy production are affected. Municipalities are one of the most important actors, because final adaptation often takes place at this level. However, planning measures is challenging for small municipalities, with adaptation capacity being lower than in big cities. A model working with data from the Global Change research Institute CzechGlobe and the Czech national drought monitor Intersucho allows for information to be obtained at the landscape scale about drought, and their utilization for small municipalities is introduced. In addition to detailed maps for the years 1991–2014, the model enables long-term prediction of drought prevalence for the years 2021–2040 and 2041–2060. GIS-integrated Random Forest regression and twelve climate, topography, and land use/land cover variables were involved in the model construction. The tuned model could explain 70% of reference data variability, and was used for drought prevalence mapping in 20 m spatial detail. Utilisation of overlay and visualisation tools and consultation of actual spatial planning maps helped create maps for spatial decision-making support in precautionary measure and landscape management within the municipalities.

Keywords: drought modelling; Random Forest; municipalities; adaptation; bivariate map; Czech Republic

Citation: Floková, L.; Mikita, T. Landscape-Scale Long-Term Drought Prevalence Mapping for Small Municipalities Adaptation, the Czech Republic Case Study. *Land* **2023**, *12*, 1937. https://doi.org/10.3390/land12101937

Academic Editor: Adrianos Retalis

Received: 22 September 2023
Revised: 10 October 2023
Accepted: 14 October 2023
Published: 18 October 2023

1. Introduction

Unlike other natural hazards, drought is characterised as a creeping event with slow development, high resilience, and long duration, tightening its grip over the area with time [1,2]. With the progress of climate change, more severe and longer drought spells are expected because of precipitation and evapotranspiration changes [3–5].

Drought is usually regarded as a water-induced phenomenon, but many other factors are taken into consideration in drought assessment, resulting in the publication of many drought concepts [6–10]. As drought represents a natural hazard and environment is a dynamic model, conceptualisation is a very important step, and end users must be considered during the whole process [11]. Applied concepts range from simplistic approaches, which employ only a single variable [3,12,13], to complex models, which combine several, mostly climatic and hydro-meteorological variables [14,15], and hybrid models, which incorporate also large-scale climate indices, to provide future scenarios for long-term drought forecasting [16]. Several reviews of drought conceptualisation can be found in the literature, e.g., [7–9,17–19].

Due to drought complexity as well as its manifold impacts, much confusion remains within the scientific and policy-making communities, a phenomenon which can lead to

indecision and inaction [20]. Nevertheless, reliable drought prevalence prediction is crucial for decision makers to provide drought preparedness plans and cope with drought [15]. Many countries are concerned about the risks connected with drought and, therefore, run national and international drought monitoring systems which serve as an information platform about drought for a wide range of users. The pioneer project is U.S. Drought Monitor, which has been operational since 1995 [14] and has been followed by other projects, e.g., the European drought observatory [21], German drought monitor [22], or Czech drought monitor Intersucho (InterDrought) [16]. The spatial resolution of these services is limited mainly due to input data availability. The U.S. drought monitor and European drought observatory uses 5 × 5 km grid, the German drought monitor operates on 4 × 4 km grid, the Czech drought monitor on a 500 × 500 m grid. The Czech Drought Monitor System Intersucho was developed in 2012 and provides near real-time soil moisture availability. It is based on four pillars [16]: (i) weekly satellite-based soil moisture estimates; (ii) daily soil moisture estimates based on the SoilClim model [23,24]; (iii) satellite-based vegetation indices; (iv) weekly in-situ expert reports.

Regardless of national initiatives and adaptation strategies, municipalities carry a legally binding responsibility of spatial planning and the final adaptation takes place mainly at the municipal level [25]. Hence, this scale is critical for effective climate adaptation [25–28]. However, most researchers focus on adaptation of built up areas, i.e., large cities [29,30], rather than on rural landscapes, which are mostly the responsibility of small municipalities [25,27,29]. Compared to the big cities, small municipalities are more vulnerable due to their lack of local adaptation capacities, i.e., scarce financial resources and workforce, limited authority and competencies, and limited access to scientific knowledge and external experts [26–28,31].

The national monitoring programmes do not provide sufficient detail for use at the municipality scale and, therefore, Geographic Information System (GIS) techniques and a multidisciplinary approach are required to better recognise the characteristics, occurrence, and effects of drought at the regional and local scale for sustainable production and land-use planning [32]. Besides climatic factors, landscape factors with high spatial variability must be involved. They are, namely, topographic characteristics and land use/land cover (LULC) characteristics. For example, vegetation coverage limits soil moisture loss, water run-off is significantly higher over steeper terrain compared to ground surface, while slope aspect determines the solar radiation which influences the hydrology of the area [33,34]. The physical coverage of the surface, which is given by land use and land cover characteristics, reflects vulnerability and possible ways of reaction in the landscape. Lately, few researchers follow multivariate approaches for local studies. Ref. [32] used the Analytical Hierarchical Process (AHP) method integrated in GIS with 13 factors—slope, elevation, aspect, soil texture, geology/lithology, LULC aggregated categories, drainage density, distance from water bodies, ground water fluctuation, normalised difference vegetation index (NDVI), see [17,35,36], rainfall, land surface temperature (LST), see [37–39], and topographic wetness index (TWI), see [39,40], to assess vulnerability to drought in the city of Kurnool, India. The study area covered approximately 8500 sq.km. Similarly, GIS-integrated AHP was applied by [33] for drought vulnerability assessment in Kangsabati Basin, India, covering an area of 9600 sq.km. Their study involved 11 factors: elevation, slope, aspect, LULC aggregated categories, population density, NDVI, LST, normalised water index, vegetation condition index, and soil moisture index. Drought modelling in Brandenburg Federal State, Germany, over an area of nearly 30 sq.km, was a subject of the work of [41]. The authors employed the GIS-based multi-criteria approach with three input parameters, NDVI, LST, and precipitation, to classify the study area in different zones of drought prevalence. Then, the agricultural and non-agricultural areas exposed and impacted with drought were quantified via overlay with LULC maps. The attempt of predicting drought without precipitation data was proposed by [34]. The authors applied Random Forest (RF) regression on 15 variables based on topography data and satellite images which characterised vegetation, topography, water, and thermal conditions in the study area. The

study area involved 12 administration units in Korea, covering approximately 3500 sq.km. Utilisation of satellite images enabled a resolution of 30 m; however, this method is useful for short-term prediction only.

The use case reflected in the proposed model enables the provision of valuable information for landscape management and sustainable land-use planning within small municipalities in the Czech Republic. The spatial detail is 20 m and the prediction is calculated for 20-year periods, 2021–2040 and 2041–2060, respectively. A supervised machine learning approach based on the RF regression implemented in GIS was used for prevalence map construction; mostly open access data were used. Climatic characteristics were created and provided by Czechglobe—Centre for Global Change Research of the Czech Academy of Science—upon a request, but similar data can be analogically created for any area from basic meteorological records and Global Circulation Models. Combination with current development plans of municipalities can reveal possible problematic areas and help target climate adaptation activities.

2. Materials and Methods

2.1. Study Area

Four study areas exhibiting different characteristics were chosen in the Czech Republic to represent the variety of landscape. They all belong to the geomorphological unit Central Moravian Carpathians, which is a part of Outer Western Carpathians. This area tends to exhibit less extreme climatic conditions when compared to other parts of the Czech Republic, and shows no significant drought hazards in the reference period 1961–2014. The prospect of drought prevalence with respect to climate change is a subject of this study. The study areas are represented by cadastral territory of five small municipalities to capture various land types and conditions (Figure 1) which can be found in this geomorphological unit.

Study area A—Sardice: occupies an area of 1729 ha, the average altitude reaches 183 m. Among all the study areas, this is the southernmost location. It is largely utilised for intensive agriculture with a high share of permanent cultivation such as vineyards and orchards, almost no forests are present. Approximately 2200 inhabitants live here.

Study area B—Prusy-Boskuvky and Vazany: to enable comparison with other study areas, two cadastral territories were merged. Both territories together occupy an area of 1317 ha and have a population of approximately 1100 inhabitants. It is the northernmost of the studied areas and the average altitude is 272 m. It is devoted mostly to fields for intensive agriculture production, very sporadic forests are present here.

Study area C—Litencice: the average altitude reaches 358 m, which is the highest value among the considered areas. The territory extends over 1053 ha and approximately 480 people live here. This study area largely consists of grassland and agricultural land with significant natural areas. Forests are present in the north.

Study area D—Korycany: the area of this territory is 1924 ha and reaches an average altitude of 280 m. More than 50% of this study area is covered with forests. In addition, an important share of agricultural land with significant natural areas can be found here; hence, this location shows the highest ecological stability of all studied regions. The population consists roughly of 2900 inhabitants.

2.2. Data

Mostly publicly available data resources were used to synthesise the database of factor layers that serve as an input for the modelling process (see Figure 2). Three groups of factors were set: climate, topography, and LULC-related.

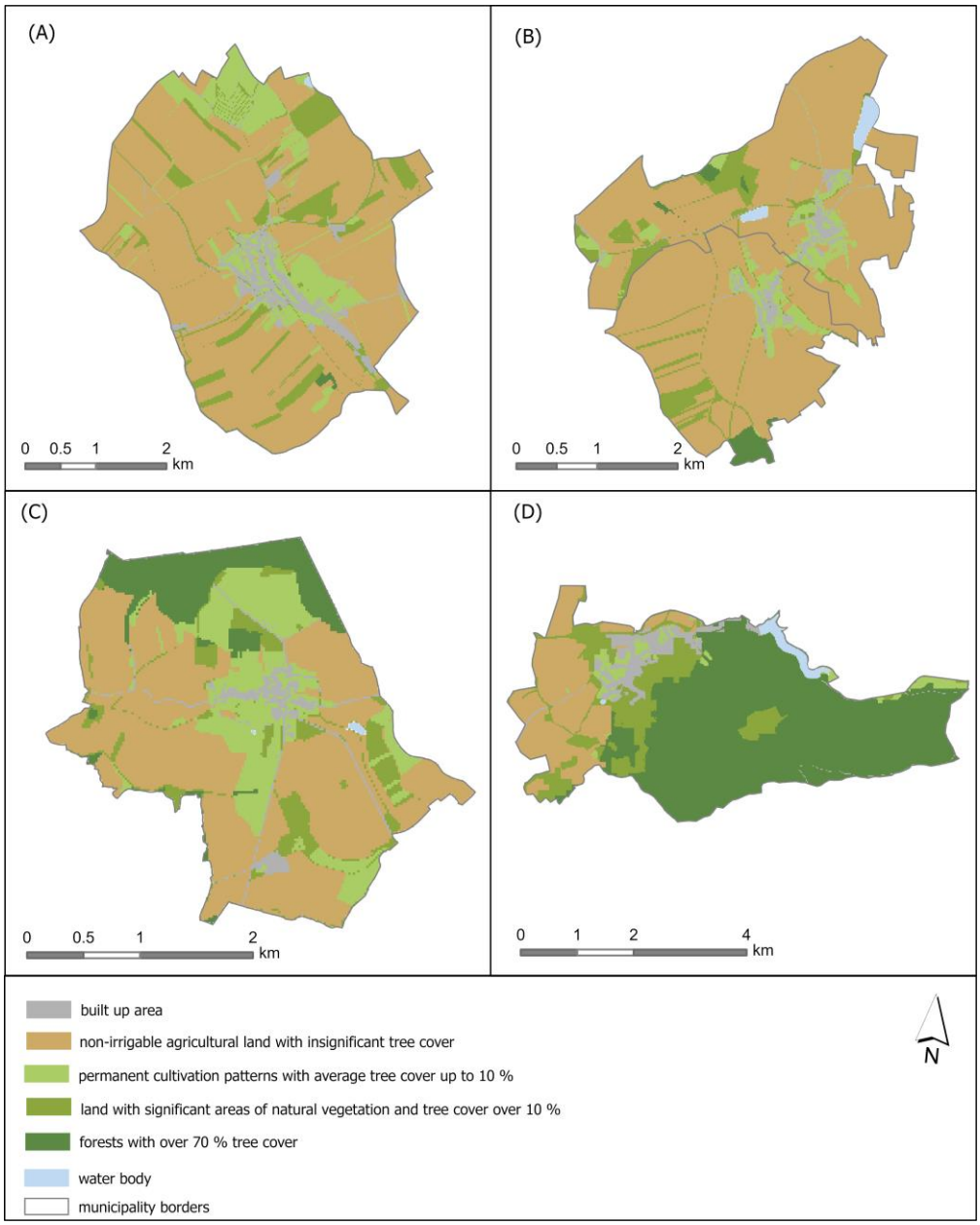

Figure 1. LULC aggregated areas for the four study areas (**A**–**D**).

Three sets of 21 layers of climatic characteristics were provided. Usually, 30-year periods as a climatic normal are used for long-term climate characteristics in a region. However, data for new climatic normal for 1991–2020 are not available yet. Climate characteristics were available for the 25-year period 1991–2014. These data were sufficient for providing the model with long-term climate characteristics of the baseline state and were preferred to currently valid climatic normal referring to years 1981–2010. Since the Czech Republic has experienced few meteorologically extreme years since 2015, such as extreme drought in 2015 and 2018, as reported by [42–44], using characteristics for 1991–2014 represents a compromise between data availability and their representativeness. The data used for modelling were created and provided by Czechglobe—Centre for Global Change Research of the Czech Academy of Science—on a basis of long–term measurements provided by the Czech Hydrometeorological Institute.

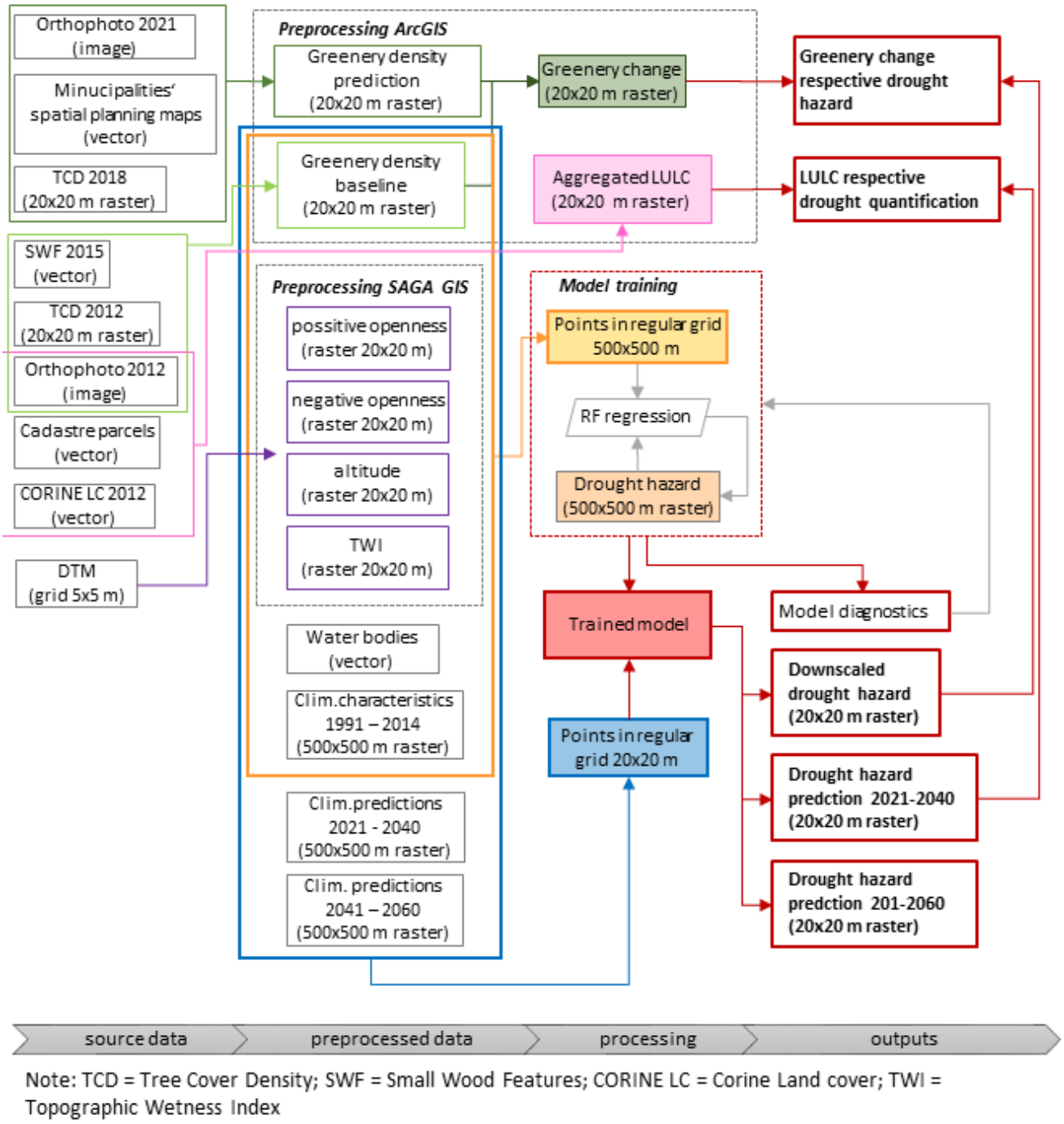

Figure 2. Structure of the source data and workflow of the model.

Climate characteristics refer to:

(i) air temperature, i.e., annual mean temperature, days with an average temperature above 10 °C in a continuous period, with a maximum temperature above 30 °C and with temperature above 5 °C;

(ii) precipitation, i.e., annual mean precipitation, mean values of precipitation in the periods between March and May, April and June, and June and August, and days with less than 1 mm of precipitation;

(iii) solar radiation, i.e., total global radiation, global radiation in the periods between March and May, April and June, and June and August, and an annual mean of global radiation;

(iv) soil moisture, i.e., moisture sufficiency at depths of up to 40 cm and 100 cm, respectively, and number of days with critically low (below 30%) soil moisture in the aforementioned depths.

Drought predictions for the periods 2021–2040 and 2041–2060 were made. For there is no suitable regional climatic model, models of the general circulation of the atmosphere coupled to an ocean model, so-called Global Circulation Models (GCMs), were utilized to produce all climatic characteristics mentioned above. According to the methodology by [45,46], data from French IPSL (Institut Pierre Simon Laplace) global climate model were used. The authors of the aforementioned studies examined 27 GCMs, and the IPSL model has proved to be closest to the median of all tested GCMs; hence, it was considered as the central model for the area of the Czech Republic. The Representative Concentration Pathway (RCP) 4.5 was adopted, as in the Fifth Assessment Report by IPCC [3] it is considered to be intermediate and the most probable scenario of greenhouse gas concentration, estimating the peak of greenhouse gases emissions (not concentration) to peak around 2040 and then decline. Climate predictions data were provided by Czechglobe—Centre for Global Change Research of the Czech Academy of Science—in 500 × 500 m grids raster layers.

Topographic characteristics were calculated based on the Digital Terrain Model (DTM) of the Czech Republic (4th generation) provided by the Czech Office for Surveying, Mapping and Cadaster. The SAGA GIS software was used for preprocessing, and ten grids were calculated referring to altitude, aspect, slope, curvature, positive openness, negative openness, catchment slope, catchment area, topography-adjusted solar radiation, and topographic wetness index (TWI).

For LULC characteristics, various source layers were compiled using ArcGIS Pro 3.0.2. These layers are important because they can capture adaptation measures. Density of the greenery in the landscape was calculated using satellite-based layers Small Woody Features (SWF) and Tree Cover Density (TCD). Based on these data, percentage in a square 100 × 100 m covered with trees and woodland shrubs was calculated. Changes in LULC were examined employing the latest orthophotos of and regional planning documents for each considered municipality to capture the climate adaptation. Development of greenery was identified, so the expected density was recalculated analogically to greenery density of the 2012 with updated input data. The difference layer of greenery change between the two study periods was created. Two layers reflecting water in the landscape were employed. On their basis, the model gathers the information about distance from a nearest water body and the shortest distance from a water stream for each modelled feature (point). For quantification of drought hazard according to LULC characteristics, a detailed vector layer of cadastre parcels referring to their use and greenery density was created. CORINE Land Cover was combined with orthophoto and detailed information about cadastre parcel use, which is registered by the Czech Office for Surveying, Mapping and Cadastre.

For the model training, reference data from the Czech national drought monitor Intersucho were employed. Drought hazard is expressed as a median of the number of days during the summer (July, August, September) with soil moisture lower than 30% in the layer up to 40 cm depth in the period 1961–2014 (considered as a climatic normal). The spatial resolution of this data is 500 × 500 m.

Unlike climatic data, the resolution of source data for topography and LULC allowed to obtain finer resolution, with grids in the spatial detail of 20 × 20 m created. Points in the regular 500 × 500 m grid possessing attributes representing all input layers and the reference attribute of drought hazard (i.e., number of days with low soil moisture) were used as input features for training the model. Points in regular 20 × 20 m grid with a detailed set of the same attributes and two more sets of climatic prediction attributes for 2021–2040 and 2041–2060 were used as features for prediction. A new number of days with low soil moisture was calculated.

2.3. Model Description

A GIS tool utilising RF regression was used for modelling in the ArcGIS Pro 3.0.2 environment; the workflow is shown in Figure 2. This method combines supervised machine learning classification or regression trees introduced by [47] and principles of bootstrap aggregation, so called "bagging" [48,49]. Randomisation (randomly selecting given number of predictor variables) included in this process enables to reduce correlation between the trees and reduce the variance in the predictions [50]. A RF method operates by creating an ensemble of decision trees (a forest) and calculating the mean of the outputs as the prediction of all the trees. Variables for the tree construction are chosen by implementing a "bagging" process; data not included in the tree construction are used for "out-of-bag" (OOB) accuracy metrics computation. Hence, no data for validation processes require exclusion during the training. On the other hand, only values used for model tuning/learning can be predicted. RF is unable to extrapolate any values outside the learned range.

Variable selection was the first step in the modelling process. In total, 41 variables regarding climate, topography, and LULC were prepared. Not all of them could be used, because a shift of climatic conditions is expected in the future. The reference (training) area had to be much larger than the study area, encompassing places covering a large portion of the variable value range, so that future values in the study area could fit within the range of available contemporary conditions of the reference dataset (see Figure 3). Variables which did not meet this requirement were excluded, as the method cannot process values not included in the training.

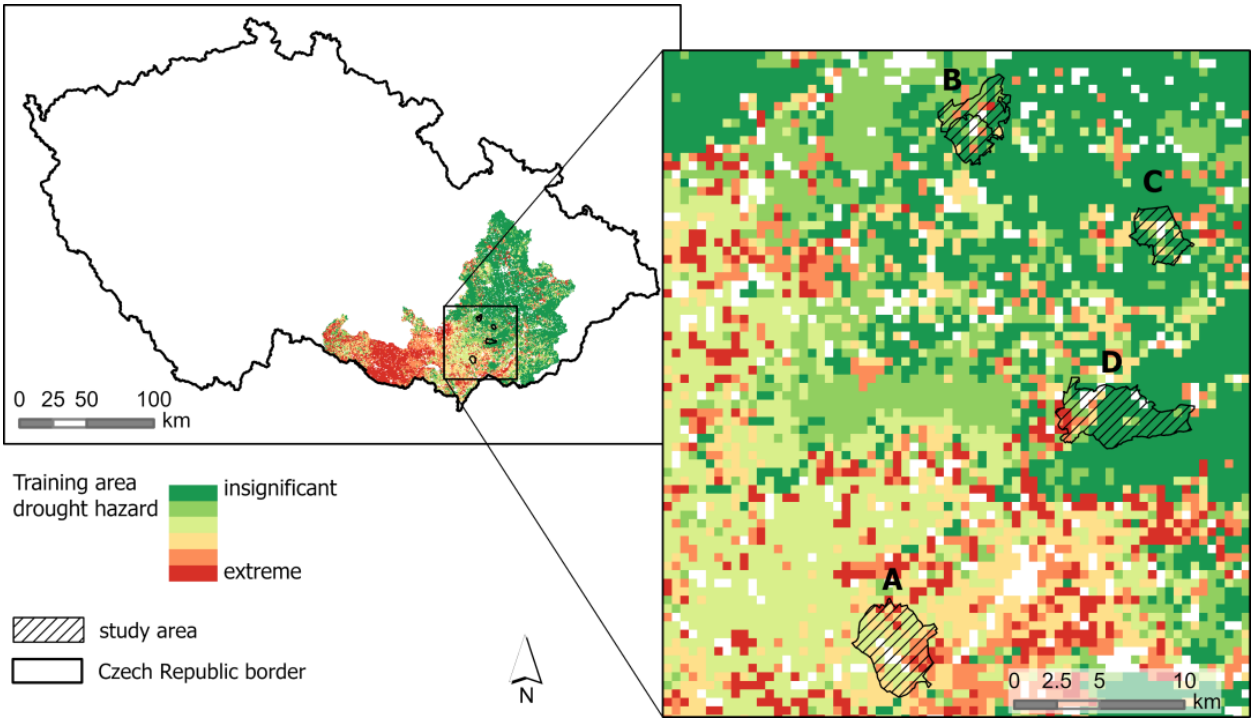

Figure 3. Drought hazard reference data for training and study areas (A–D).

Further variable selection was conducted via a variable importance metric [50]. The variable importance (VI) metric is calculated for each variable during each run of the RF model based on the reduction in the sum of squared errors (out-of-bag, OOB errors) whenever a variable is chosen to split the tree. Each category of variables was reduced by omitting the least significant factors, with only the top 40% in each category retained. In total, twelve variables were chosen for model construction: six climate characteristics, four topography-related characteristics, and two LULC-related characteristics. Factors involved in the model and their importance are shown in Table 1.

Table 1. Variables and their variable importance for the model.

Variable	VI
Annual mean of global radiation	19%
Number of days with an average temperature above 5 °C in a continuous period	12%
Mean values of precipitation in the periods June to August	11%
Annual mean precipitation	11%
Mean values of precipitation in the periods March to May	10%
Total global radiation	9%
Altitude	8%
Distance from water bodies	4%
Density of greenery	4%
Positive openness	4%
Negative openness	4%
Topographic wetness index (TWI)	4%

Removing variables with a lower importance did not degrade the model performance; on the contrary, model performance slightly improved after variable optimisation. Although climatic variables showed the highest importance, there was an urge to involve all three categories of factors, because unlike climatic factors, topography- and LULC-related variables can bring higher spatial detail owing to their higher spatial variability. Model-based optimisation was used for hyperparameter tuning of the model [51]. The number of trees was found to be the most important. It was gradually increased to 2000 when low variability in the VI metric of individual predictors was reached. Low variability indicates the model stability and, hence, reduces uncertainty in outputs.

Number of trees have proved to be important also for model accuracy. The Root Mean Squared Error (RMSE) and coefficient of determination R-squared (R2) were used for evaluation of the model accuracy progress. Both these measures are useful when describing model performance. RMSE explains the predictive ability of the model in absolute terms: the lower the RMSE, the better. The R-squared value expresses how well the variability in the dependent variable is explained by a given model, with higher R-squared values desirable. These measures were derived from OOB error, which is based on data not included in the construction of individual trees in a given forest (unseen data). The development of RMSE and R-squared is shown in Figure 4. RMSE decreased significantly with an increasing number of trees, which means the error was lower when using more trees for prediction. On the contrary, R-squared increased with an increasing number of trees, suggesting that the model with more trees can better capture the variability in the input data. In conclusion, the higher the number of trees used for model training, the more accurate the result. The training was stopped at 2000 trees as the curves reached a plateau, with the addition of more trees failing to engender a significant improvement in the model. The RMSE of the model with 2000 trees was 5.8 and R-squared was 0.71.

Besides OOB error diagnostics, a validation using independent training and testing datasets was used. The difference between OOB error and validation using separate testing and training datasets is that, not only trees constructed with unseen data (see above) but entire forests could be used for validation. Thirty percent of input points were set aside as validation data. The performance of training and testing datasets in the model containing 2000 trees is displayed in Table 2.

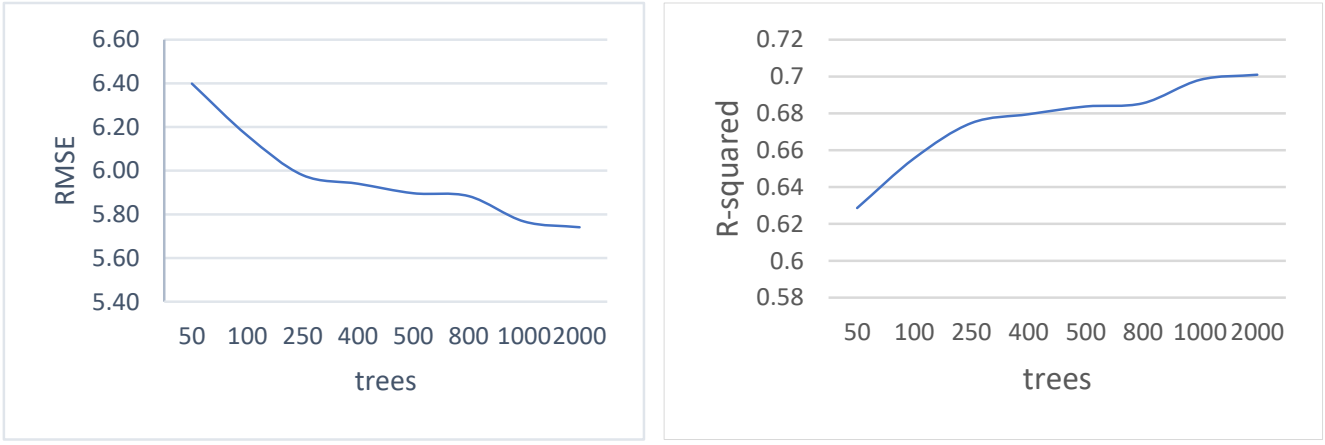

Figure 4. Changes in RMSE values (**left**) and R-squared values (**right**) based on the number of trees.

Table 2. Model performance for training and testing subsets.

	R2	*p*-Value	Standard Error
Training	0.951	0.000	0.001
Testing (mean value)	0.700	0.000	0.004

The selection of the validation dataset is random, and the validation diagnostics can differ in values across runs. Hence, the model was run iteratively 30 times. The average value of R-squared was 0.70, which means that the model could explain 70% of variability in the test dataset. The distribution of R-squared across the 30 runs of the model is displayed in Figure 5.

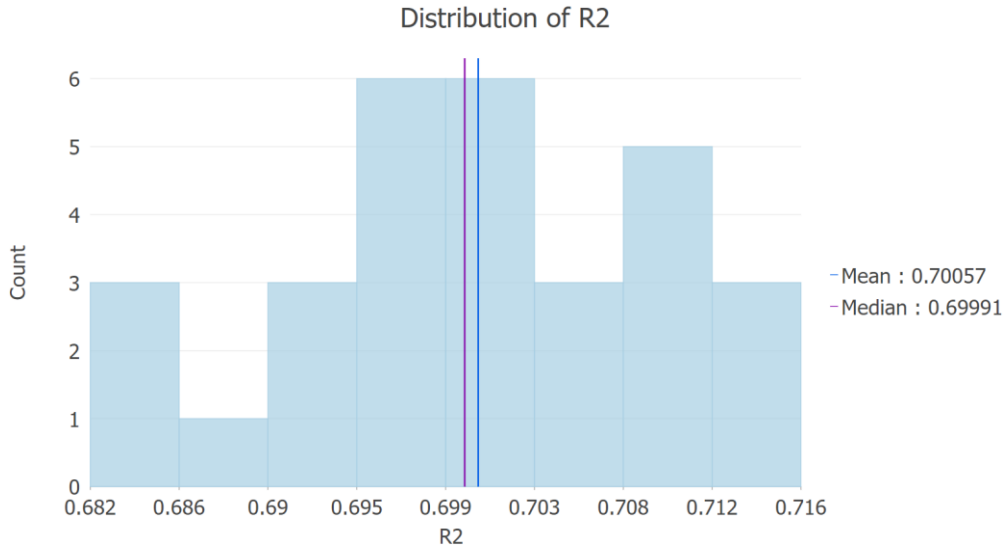

Figure 5. Distribution of R-squared (R2) during 30 runs of the model with the validation dataset.

For environmental models are highly case-specific, the suitability of the actual dataset and the given area of interest were further examined. Residual analysis was used to evaluate the model effectiveness. Figure 6 displays the distribution of raw residuals and standardised residuals within the study area. In both cases, normal distribution can be seen. Raw residuals show the difference between predicted and reference data in days.

Standardised residuals were calculated according to Equation (1) and measure the strength of the difference between reference and predicted values.

$$standardised\ residual = reference\ value - predicted\ value / \sqrt{predicted\ value} \quad (1)$$

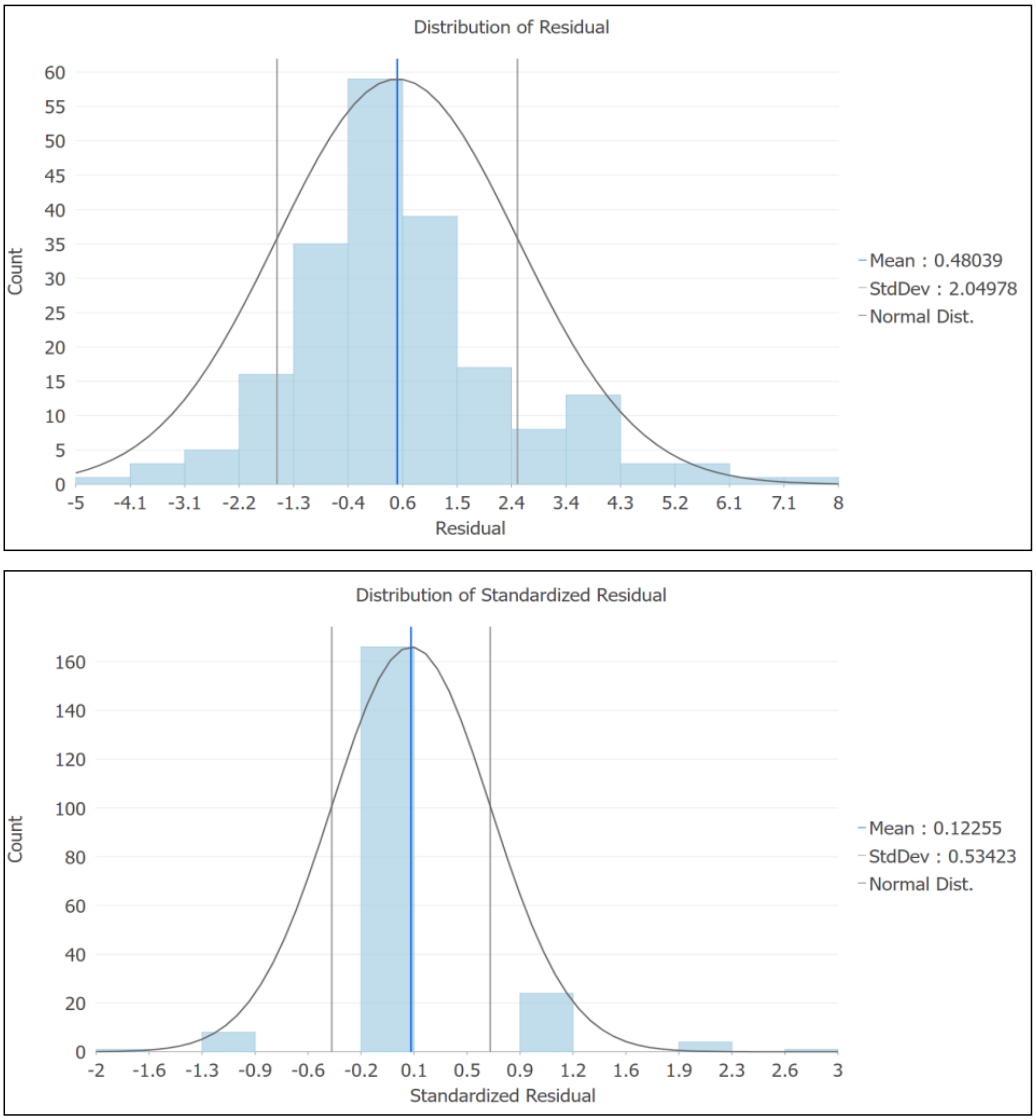

Figure 6. Distribution of raw (**above**) and standardised residuals (**bottom**) within the study area.

Standardised residuals should fit within the range of $[-2, 2]$. Values outside this range indicate the presence of outliers. No outliers were identified in the dataset of the study area.

The spatial distribution of standardised residuals throughout the study area is illustrated in Figure 7.

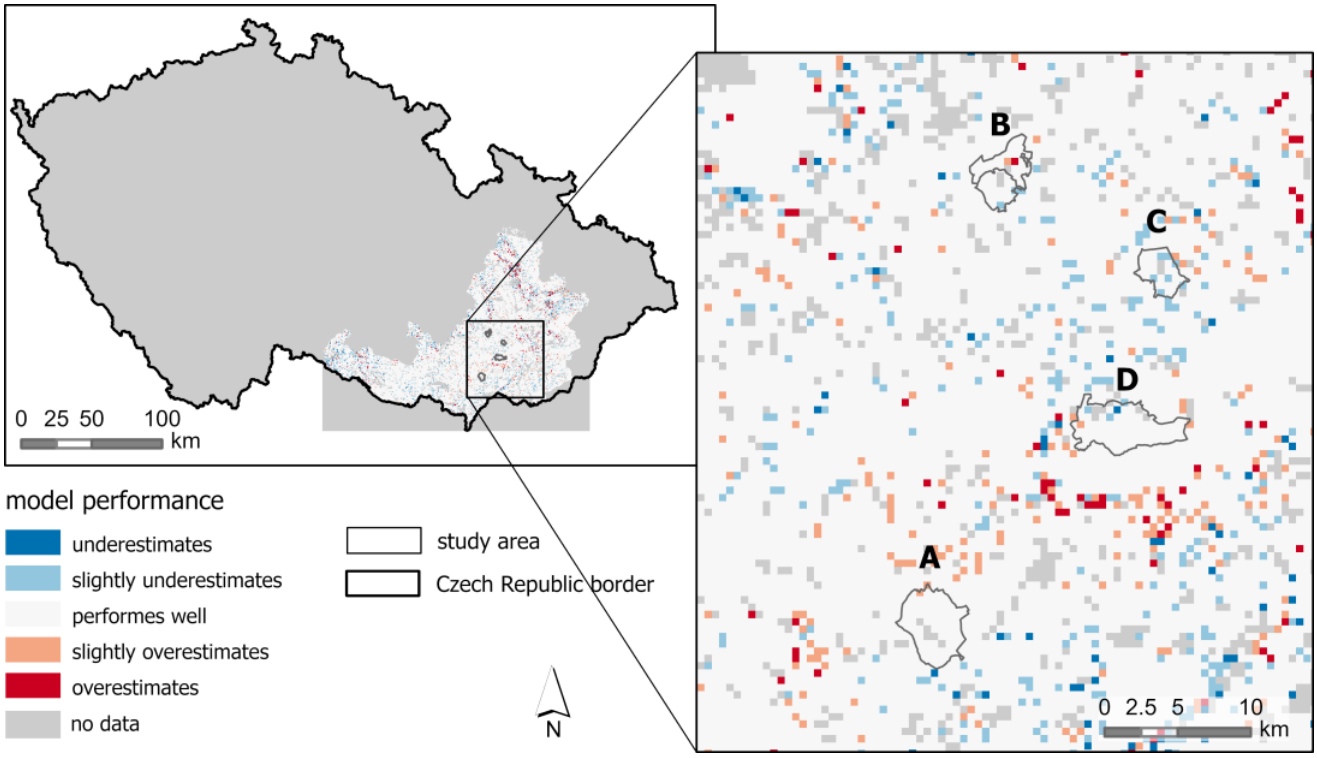

Figure 7. Spatial distribution of standardised residuals, letters A–D refer to the study areas.

The final RF regression model, which uses an ensemble of 2000 trees, was established. This model employs 12 variable predictors, for each of them a VI was calculated (Table 1). Training of the model was achieved with the utilisation of over 40,000 points in a regular grid 500 × 500 m covering the entire training area and having the attributes of all prediction variables and known value of long-term drought hazard stated by the Czech national drought monitor Intersucho. After the training, downscaling was processed using a finer fishnet with almost 140,000 points in a regular grid 20 × 20 m covering all the investigated municipalities. For these points, having the same prediction variables but based on finer scale layers where available, the model assessed the values of drought hazard with respect to the rules learned from the training stage. Consequently, with the use of climatic predictions data derived from IPSL GCM, prediction of drought hazard for the periods 2021–2040 and 2041–2060 were created.

3. Results

Three main outputs were created, mostly in the form of specialised maps.

3.1. Drought Prevalence Development

One of the main model outputs was an ensemble of drought prevalence maps for the periods 1991–2014, 2021–2040, and 2041–2060 with a spatial resolution of 20 m (Figure 8). There was an obvious shift in drought prevalence in all studied areas. Six drought categories were established using a natural break method according to a predicted number of days when soil moisture was lower than 30% in the layer up to 40 cm depth during the months of July, August, and September.

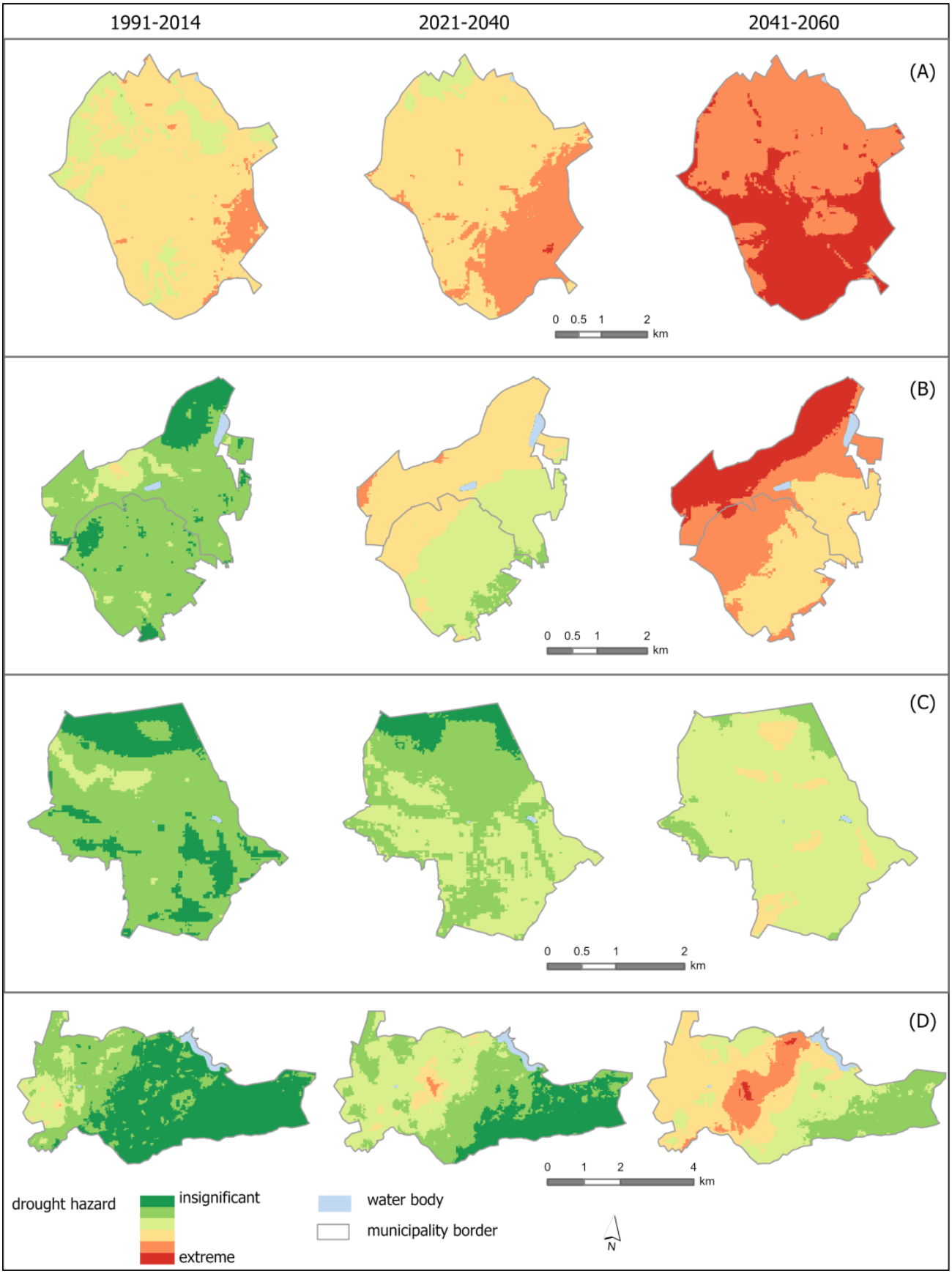

Figure 8. Predicted long-term drought prevalence in the study areas (**A**–**D**).

The study area A shows the highest drought hazard in all periods. With respect to the 1991–2014 period, the whole municipality was found to exhibit moderate to strong drought hazard. The hazard developed even more with the continuous climate change, with the area of strong drought hazard expanding further southeast in 2021–2040. This trend continued in the period 2041–2060, with most of the southern part, which is mainly devoted to fields, becoming exposed to the extreme drought hazard. The central and northern part have a higher share of permanent cultures such as vineyards and orchards and showed a slightly lower drought hazard.

Even more dramatic shifts in drought hazard can be noticed in the study area B. Similarly to A, this municipality consists mainly of fields for intensive agricultural production. The drought hazard in 1991–2014 was found to be insignificant, with only a small area of moderate drought hazard being visible in the northwest. However, drought expands rapidly from the northwest. For the period 2041–2060, the drought hazard was predicted to occur in all areas, reaching extreme values in the northwest part.

An insignificant drought hazard was identified in the study area C during 1991–2014, but moderate drought was found to occur during the period 2021–2040 in the south, especially in the parts which are not devoted to permanent cultivation. The lowest hazard of drought was predicted to characterise forests in the north. With respect to the period 2041–2060, a moderate drought hazard was predicted for almost all areas, with small patches of higher drought hazard occurring. The lowest drought hazard from all studied municipalities appeared in the study area D. With respect to the period 1991–2014, most of the investigated area showed insignificant or very low drought hazard, especially the forests, which cover the eastern part of the region. Only small places with moderate drought were found to 4occur in the west. This area is mostly devoted to intensive agricultural production. The prediction for 2021–2040 showed that the western part is expected to become drier, but places with very high drought hazard appeared in the central part. This trend continued through 2041–2060; a high drought hazard is expected in the western part, while a very high hazard of drought was observed in the valley in the central part, which is a place of settlement and other human activities.

3.2. Land Use/Land Cover Respective Drought Hazard Quantification

To quantify the results, zonal statistics for aggregated LULC categories was calculated. Five groups (see Figure 1) were created depending on the LULC and share of tree cover. LULC categories differ in their adaptation capacity, which affects the overall vulnerability of the area. For each category, the share of area exposed to very high or extreme drought hazard was stated (see Table 3). Very high or extreme drought hazard (orange and red category in Figure 8) means that the soil moisture is less than 30% in the layer up to 40 cm during the months of July, August, and September for 20 or more days cumulatively.

Table 3. LULC aggregated categories and their proportion in percent (and area in hectares) endangered by very high or extreme drought hazard in the modelled periods.

LULC Category	1991–2014	2021–2040	2041–2060
built-up area	3.4% (9 ha)	7.8% (21 ha)	44.6% (122 ha)
non-irrigable agricultural land with insignificant tree cover	3.0% (88 ha)	7.2% (210 ha)	62.6% (1828 ha)
permanent cultivation patterns with average tree cover up to 10% and build up area	1.2% (6 ha)	3% (15 ha)	50.0% (257 ha)
agricultural land with significant areas of natural vegetation and tree cover over 10%	0.6% (4 ha)	3.5% (22 ha)	49.5% (312 ha)
forests and land with over 70% tree cover	0.01% (0.2 ha)	0.6% (7 ha)	17.8% (222 ha)

In conclusion, the predicted prevalence of drought is more severe in municipalities located in lowlands, where most of the land is used for seasonal agricultural production. Permanent cultures show lower hazard and areas covered with forest tend to be the least endangered. This data reflects generally accepted facts, that grown trees and bushes can positively affect the microclimate in the surroundings and mitigate drought development. Permanent cultures such as gardens, vineyards, orchards, and even permanent grasslands exhibit greater resistance also because of a deeper rooting system compared to seasonal crops in fields. Moreover, fields are left bare at least during part of the year, which has a significant negative impact on the thermal and moisture regime in the soil and the microclimate. Data also show that by retaining contemporary LULC and as a result of the expected progress of climate change, approximately 50% of agricultural land might face very high drought hazard by 2040, although they have not been endangered recently.

3.3. Adaptation Measure Planning

Spatial planning and landscape management are crucial tools that can provide guidance for land use, facilitating climate change adaptation [52]. One of the best ways to integrate climate change into spatial planning is through usage of visualisation tools [53,54]. The detailed mapping of drought prevalence can help understand specific landscape conditions. Spatial analysis of the drought hazard was combined with the spatial planning of the individual municipality development plans.

Two-variable (bivariate) maps were created [55] using two variables, i.e., drought hazard and planned development of greenery (Figure 9). Each variable is represented by a specific colour scheme and the resulting colour is determined as a mixture of colours obtained from these colour scales for given values of variables [56]. The relation between variables can be compressed into a single image, instead of creating two separate images which the user needs to overlay mentally. Maps displayed in Figure 9 capture the relationship of the predicted drought hazard in the period 2021–2040, as well as changes in tree and woodland shrub cover. These changes either have been realised since the baseline 2012 or are planned for the near future, and refer mainly to the construction of biocentres and biocorridors as part of the Territorial System of Ecological Stability. Although biocentres and biocorridors are not originally intended as climate adaptation and mitigation measures, synergy of the landscape management activities is desirable. The blue scale indicates changes in tree and shrub cover from no development to moderate and high development, whilst the drought hazard is displayed with a red scale ranging from low hazard to moderate and high hazard of drought. Hence, places with low drought hazard and a low degree of change in greenery density can be identified as white areas typically representing forests, whilst red areas indicate places with high drought hazard and no progress in greenery density. Attention should be paid to the latter when planning adaptation activities, as they are highly exposed to the drought hazard and have low adaptation capacity but are omitted from any measures. On the other hand, purple and dark purple areas represent places with significant drought hazard but also expected high development in tree and shrub cover. The greenery development here successfully targets places with high drought hazard to moderate the drought impact in the area. However, this holds true for fully-grown trees and shrubs. It is necessary to pay special attention to the species selection, and care is required to ensure newly planted trees and shrubs in these areas are able to reach maturity.

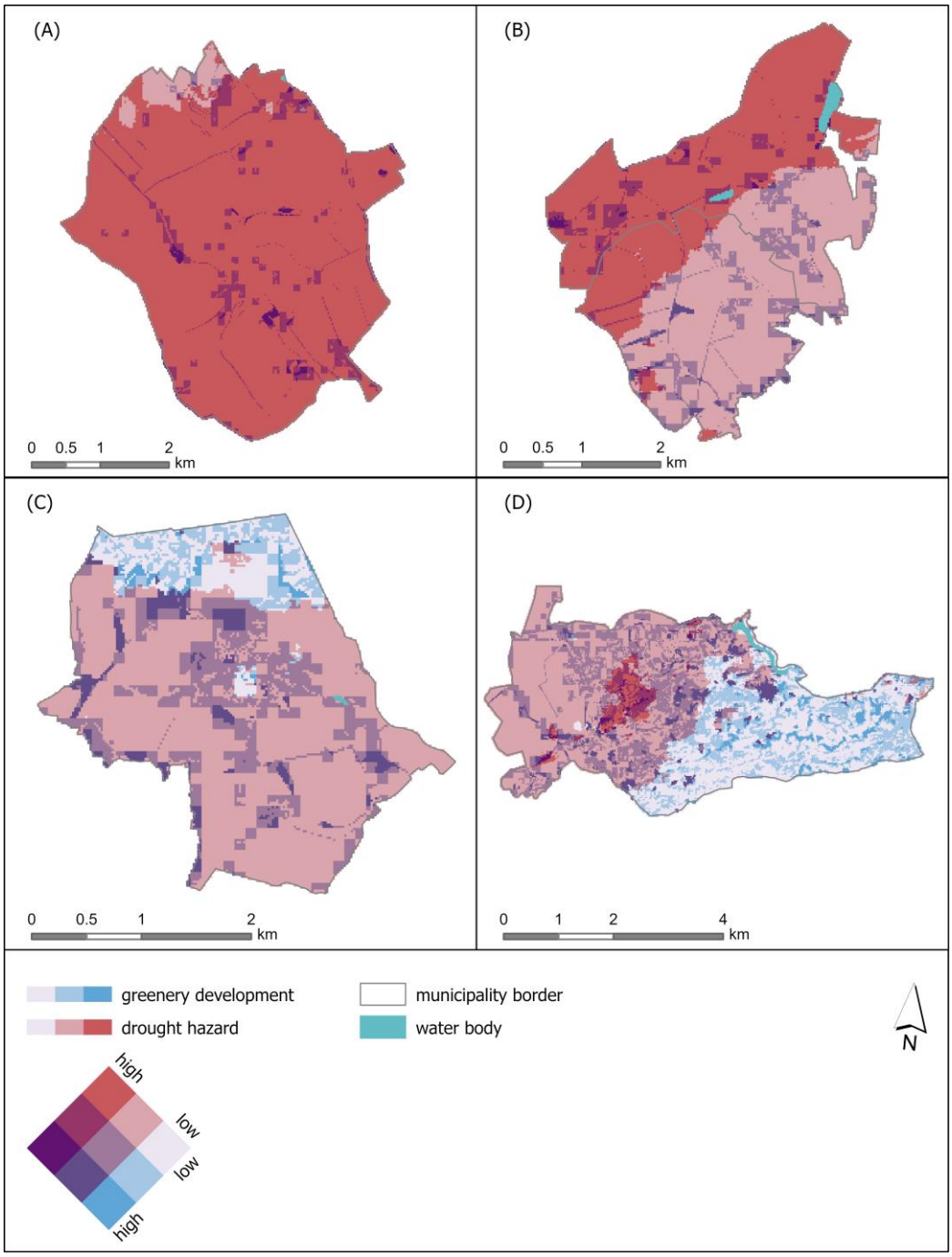

Figure 9. Relation of predicted drought hazard and greenery development in the period 2021–2040 for study areas (**A**–**D**).

4. Discussion

4.1. Model Application

Downscaled drought prevalence maps at the 20 m resolution were obtained. In addition, the importance of factors responsible for drought hazard occurrence can be stated on the basis of model diagnostic. Three groups of factors were involved, i.e., climatic, topographic, and LULC factors. Climatic factors were found to be the most significant. Taking action in this area involves mitigation measures regarding decarbonisation and green city models. Nevertheless, these are not drought-specific measures and climate policy of local government does not have the same global power as national ones [57]. Topographic factors are difficult or even impossible to change. Hence, despite the fact,

that LULC factors appear to be the least significant for model prediction, they are pivotal for small municipalities' agenda setting. Unfortunately, municipalities, instead of acting preventively, they tend to accept pragmatic and responsive measures [27].

Effective adaptation should follow three main steps—(i) problem identification, (ii) political decision-making and strategic management, and (iii) realisation of measures [28,58]. However, small municipalities face several obstacles in this process. Some papers have been produced on this topic and conclude that among the most frequent barriers are low awareness or relevance of climate change compared to other issues, lack of expertise, insufficient competencies, and limited financial sources [25,27,28,58,59]; technical problems are also mentioned [58,60]. High-resolution hazard maps are considered to be an important tool for climate adaptation activities [60].

The long-term drought prevalence maps presented herein for different periods reveal trends in drought development and can help with hazard identification. The implementation of overlay and visualisation techniques enable the creation of resources, affording support to decision-makers in the development of preventative policies to address future drought impacts. The example presented in this study deals with the relationship of drought hazard development and greenery planning managed by the local government. Greenery planning takes place only at common property places. For the realisation of wider measures it is important to involve all stakeholders such as farmers, land owners, citizen groups, and local community [30,61–64]. An analysis of drought hazard development in relation to owner structure can be used. On this basis, revision of tenancy agreements and pressure on the municipality property tenants can be applied. Active dialog with actors and society to raise awareness and promote understanding of the need for action can be initialised. Only then wider landscape adaptations, revitalisations, and changes in crop management and farming regimes can be implemented to improve the water regime, state of the landscape, and its overall resilience.

4.2. Model Limits

The RF algorithm implemented in the GIS environment was used for model construction. This method belongs to the class of data-driven models and can work either as RF regression or RF classification. In this case, RF regression was used. A similar method was used for short-term drought prediction by [34]. There are many advantages associated with usage of RF modelling described in the literature, e.g., models can capture non-linear dependencies between predictor and dependent variables [65], simultaneously continuous and categorical variables can be incorporated [66], models can handle highly correlated predictor variables [65,67], as well as exhibiting a tendency not to overfit [34,66]. On the other hand, there are some limits, which cannot be omitted. RF cannot adequately model datasets with imbalanced data [68] and is unable to extrapolate values outside the training range [69]. In this study, this problem was overcome by utilising a much bigger training area, so that shifts in future climatic data predictions could be involved in the learning process. This is possible only if there are enough places which today comply with the future conditions expected in the study areas. This fact can often be limiting.

Another advantage of RF is its ability to determine individual variable importance. However, RF, as all algorithmic models, performs as a black-box, so the variable importance should be considered carefully [34]. It is unknown whether the correlation between the drought risk and variable importance is positive or negative.

RF is based on the statistical evaluation of different combinations of factors and dependent variable. The accuracy of the downscaling corresponds to the validation of the model. The rules that the model learns during the training are applied to entities placed in a finer fishnet of points, with the spatial detail carried by the higher resolution of input layers (updated attributes), such as detailed LULC and topography characteristic. Nevertheless, certain limits are connected with reference data used for training. Long-term drought characteristics from the drought monitoring programme Intersucho are derived from regional-scale programme models of evapotranspiration and soil moisture on the

basis of a robust model, SoilClim [16,23,24,70], which takes into account soil characteristics, type and phenology of vegetation cover, LULC, snow cover accumulation, and melting. It may be argued that not all of the relations in microclimate can be clearly revealed on the basis of the regional model data. For example, the proposed RF regression model showed that the importance of greenery density and waterbody proximity was lower than expected based on experience and a literature review [71–73]. Similar conclusions were reached by [34], who also used a RF regression model. Proposed outputs can be used for preventative measures as presented in this study, but other methods, such as multi-linear regressions, should be used, or other experts or studies should be referred to in order to obtain a deeper understanding of factor importance [34].

Another source of uncertainty is the usage of global circulation models (GCMs) for scenario development (prediction). This uncertainty issue was dealt with by [74] in a study from the Washington state (US). However, due to a lack of detailed data of future climate conditions, GCMs are used for local studies too, e.g., for regions of the Czech Republic [24,75], Edwards Plateau (Texas, US) [76], and Centre-du-Québec (Canada) [77]. To reduce uncertainty, ensembles of models are often employed for modelling scenarios [76,77]. In some cases, individual models are evaluated and data from the model which performs best [78] or from a central model (closest to median value), e.g., this study and [46], are employed.

The proposed model captures trends in drought development and its spatial distribution suitably, thus supporting spatial decision-making. Nevertheless, modelling of the exact impact of individual changes in the landscape is a subject for future research and would require further expertise and detailed information of LULC, landscape patterns, and soil moisture [79].

5. Conclusions

Drought is one of the most threatening hazards connected with climate change. Preparedness of different actors will be crucial for the development and implementation of climate adaptation measures. These actions cannot be conducted without conceptual planning based on high-resolution information systems [80]. Many research projects about drought focus on specific fields such as agriculture, forestry, hydrology, etc. Municipalities are key players, as they contribute to climate action policy, but they are also affected by the impacts of drought [3,28,57]. This is very challenging, especially for small municipalities which face obstacles due to limited budget, lack of human resources or insufficient access to scientific knowledge [25,27,28,59].

National or international drought services provide long-term monitoring, but the spatial resolution of these data does not fully meet the requirements for applicability to local purposes. This study presents a model which enables the downscaling of the national drought monitor data Intersucho to the scale suitable for decision-making relative to landscape management and land-use planning at the municipality scale. The input datasets for this model were developed mostly with publicly available data. By employing GCM climatic data prediction, the model enables prediction of future trends in the development of drought prevalence with regard to climate change.

The RF regression model was created in ArcGIS Pro 3.0.2 environment. Twelve factors related to climate, land use/land cover, and topography characteristics were employed. The model was implemented in four areas of interest, which were chosen to capture landscape variability with respect to the geomorphological unit Central Moravian Carpathians. Long-term drought characteristics for the years 1961–2014 from the national drought monitor Intersucho were used for training, 2000 trees were created, and almost 40,000 reference points were involved in the training process. The model could explain 70% of data variability on average.

A finer detail of drought prevalence was modelled employing finer LULC and topographic data, and future trends in drought development were obtained on the basis of IPSL global circulation model predictions for representative concentration pathway 4.5 scenario. Even though the studied areas are not regarded as drought hazard areas, an increasing risk of drought hazard is obvious in all of them. A more dramatic progression can be expected in municipalities occupying lowland with significant shares of arable land, whilst lower hazard is predicted in municipalities with high shares of forests and woodland cover located in higher altitude.

Quantification of drought hazard regarding individual LULC categories is also provided. Arable land with low shares of tree cover show the highest rise in drought hazard, whilst forests and areas with significant tree cover show low rise of drought hazard.

Implementation of model outputs decision-making at the municipality level is suggested. In addition to development plans and bivariate visualisation techniques, detailed maps of relationship in greenery development and drought hazard development were created. Places with high drought hazard and no increase in greenery density can be easily identified as well as areas with high greenery development, which will face significant drought. Such information is important for sustainable landscape management planning.

Even though the model is created for Central Moravian Carpathians, the method can be used for other regions as long as the data is available. Transferability of the method is supported by using mostly publicly available data.

Author Contributions: Conceptualization, L.F. and T.M.; methodology, L.F. and T.M.; validation, L.F.; resources, L.F. and T.M.; data curation, L.F.; writing—original draft preparation, L.F.; writing—review and editing, T.M.; visualization, L.F.; supervision, T.M. All authors have read and agreed to the published version of the manuscript.

Funding: This research received no external funding.

Data Availability Statement: Most data are publicly available via Czech Office for Surveying, Mapping and Cadastre: https://ags.cuzk.cz/geoprohlizec/?k=11272 (accessed on 15 November 2022), https://ags.cuzk.cz/geoprohlizec/?p=79, https://services.cuzk.cz/shp/ku (accessed on 15 November 2022). Or via European Environmental Agency Copernicus Land Monitoring Service: https://land.copernicus.eu/pan-european/high-resolution-layers/small-woody-features (accessed on 15 November 2022), https://land.copernicus.eu/pan-european/corine-land-cover/clc-2012 (accessed on 15 November 2022), https://land.copernicus.eu/pan-european/high-resolution-layers/forests/tree-cover-density (accessed on 15 November 2022). Some data were provided by a third party and are available upon a request.

Acknowledgments: We thank Czechglobe—Centre for Global Change Research of the Czech Academy of Science for the climatic data provided for the purpose of this study.

Conflicts of Interest: The authors declare no conflict of interest.

References

1. Spinoni, J.; Naumann, G.; Vogt, J.V. Pan-European seasonal trends and recent changes of drought frequency and severity. *Glob. Planet. Chang.* **2017**, *148*, 113–130. [CrossRef]
2. Mishra, A.K.; Desai, V.R. Drought forecasting using stochastic models. *Stoch. Environ. Res. Risk Assess.* **2005**, *19*, 326–339. [CrossRef]
3. IPCC. *Climate Change 2014: Synthesis Report. Summary for Policymakers*; Pachauri, R.K., Meyer, L.A., Eds.; IPCC: Geneva, Switzerland, 2014; ISBN 9781139177245.
4. Hoegh-Guldberg, O.; Jacob, D.; Taylor, M.; Bindi, M.; Abdul Halim, S.; Achlatis Australia, M.; Waterfield, T. Hubertus Fischer (Switzerland), Klaus Fraedrich (Germany), Sabine Fuss (Germany). Global Warming of 1.5 °C. An IPCC Special Report on the Impacts of Global Warming of 1.5 °C Above Pre-Industrial Levels and Related Global Greenhouse Gas Emission Pathways, in the Context of Strengthening the Global Response to the Threat of Climate Change. 2018. Available online: https://www.ipcc.ch/site/assets/uploads/sites/2/2019/02/SR15_Chapter3_Low_Res.pdf (accessed on 22 February 2022).
5. Samaniego, L.; Thober, S.; Kumar, R.; Wanders, N.; Rakovec, O.; Pan, M.; Zink, M.; Sheffield, J.; Wood, E.F.; Marx, A. Anthropogenic warming exacerbates European soil moisture droughts. *Nat. Clim. Chang.* **2018**, *8*, 421–426. [CrossRef]
6. Dai, A. Drought under global warming: A review. *Wiley Interdiscip. Rev. Clim. Chang.* **2012**, *3*, 45–65. [CrossRef]

7. Eslamian, S.; Ostad-ali-askari, K.; Singh, V.P.; Dalezios, N.R. A Review of Drought Indices. *Int. J. Constr. Res. Civ. Eng.* **2017**, *3*, 48–66. [CrossRef]
8. Hao, Z.; Singh, V.P.; Xia, Y. Seasonal Drought Prediction: Advances, Challenges, and Future Prospects. *Rev. Geophys.* **2018**, *56*, 108–141. [CrossRef]
9. Mishra, A.K.; Singh, V.P. A review of drought concepts. *J. Hydrol.* **2010**, *391*, 202–216. [CrossRef]
10. Svoboda, M.; LeComte, D.; Hayes, M.; Heim, R.; Gleason, K.; Angel, J.; Rippey, B.; Tinker, R.; Palecki, M.; Stooksbury, D.; et al. The drought monitor. *Bull. Am. Meteorol. Soc.* **2002**, *83*, 1181–1190. [CrossRef]
11. Hayes, M.; Svoboda, M.; Wall, N.; Widhalm, M. The lincoln declaration on drought indices: Universal meteorological drought index recommended. *Bull. Am. Meteorol. Soc.* **2011**, *92*, 485–488. [CrossRef]
12. Vicente-Serrano, S.M.; Beguería, S.; López-Moreno, J.I. A multiscalar drought index sensitive to global warming: The standardized precipitation evapotranspiration index. *J. Clim.* **2010**, *23*, 1696–1718. [CrossRef]
13. Yu, H.; Zhang, Q.; Xu, C.Y.; Du, J.; Sun, P.; Hu, P. Modified Palmer Drought Severity Index: Model improvement and application. *Environ. Int.* **2019**, *130*, 104951. [CrossRef] [PubMed]
14. Svoboda, M. An Introduction to the Drought Monitor University of Nebraska—Lincoln DigitalCommons @ University of Nebraska—Lincoln An Introduction to the Drought Monitor. *Drought Netw. News* **2000**, *80*. Available online: https://digitalcommons.unl.edu/droughtnetnews/80 (accessed on 17 March 2023).
15. Hao, Z.; Hao, F.; Singh, V.P. A general framework for multivariate multi-index drought prediction based on Multivariate Ensemble Streamflow Prediction (MESP). *J. Hydrol.* **2016**, *539*, 1–10. [CrossRef]
16. Trnka, M.; Hlavinka, P.; Možný, M.; Semerádová, D.; Štěpánek, P.; Balek, J.; Bartošová, L.; Zahradníček, P.; Bláhová, M.; Skalák, P.; et al. Czech Drought Monitor System for monitoring and forecasting agricultural drought and drought impacts. *Int. J. Climatol.* **2020**, *40*, 5941–5958. [CrossRef]
17. Zargar, A.; Sadiq, R.; Naser, B.; Khan, F.I. A review of drought indices. *Environ. Rev.* **2011**, *19*, 333–349. [CrossRef]
18. Mishra, A.K.; Singh, V.P. Drought modeling—A review. *J. Hydrol.* **2011**, *403*, 157–175. [CrossRef]
19. Crocetti, L.; Forkel, M.; Fischer, M.; Jurečka, F.; Grlj, A.; Salentinig, A.; Trnka, M.; Anderson, M.; Ng, W.T.; Kokalj, Ž.; et al. Earth Observation for agricultural drought monitoring in the Pannonian Basin (Southeastern Europe): Current state and future directions. *Reg. Environ. Chang.* **2020**, *20*, 123. [CrossRef]
20. Wilhite, D.A.; Glantz, M.H. Understanding: The drought phenomenon: The role of definitions. In *Water International*; Taylor and Francis: Oxfordshire, UK, 1985; Volume 10, pp. 111–120. ISBN 9781000232257.
21. European Comission. Combined Drought Indicator (CDI) v2; European Drought Observatory: 2022. Available online: https://edo.jrc.ec.europa.eu/ (accessed on 18 March 2023).
22. Zink, M.; Samaniego, L.; Kumar, R.; Thober, S.; Mai, J.; Schäfer, D.; Marx, A. The German drought monitor. *Environ. Res. Lett.* **2016**, *11*, 074002. [CrossRef]
23. Hlavinka, P.; Trnka, M.; Balek, J.; Semerádová, D.; Hayes, M.; Svoboda, M.; Eitzinger, J.; Možný, M.; Fischer, M.; Hunt, E.; et al. Development and evaluation of the SoilClim model for water balance and soil climate estimates. *Agric. Water Manag.* **2011**, *98*, 1249–1261. [CrossRef]
24. Štěpánek, P.; Trnka, M.; Chuchma, F.; Zahradníček, P.; Skalák, P.; Farda, A.; Fiala, R.; Hlavinka, P.; Balek, J.; Semerádová, D.; et al. Drought prediction system for central europe and its validation. *Geosciences* **2018**, *8*, 104. [CrossRef]
25. Slavíková, L.; Raška, P.; Kopáček, M. Mayors and "their" land: Revealing approaches to flood risk management in small municipalities. *J. Flood Risk Manag.* **2019**, *12*, 12474. [CrossRef]
26. Vogel, B.; Henstra, D. Studying local climate adaptation: A heuristic research framework for comparative policy analysis. *Glob. Environ. Chang.* **2015**, *31*, 110–120. [CrossRef]
27. Buschmann, D.; Koziol, K.; Bausch, T.; Reinhard, S. Adaptation to climate change in small German municipalities: Sparse knowledge and weak adaptive capacities. *Nat. Resour. Forum* **2022**, *46*, 377–392. [CrossRef]
28. Kopp, J.; Kureková, L.; Hejduková, P.; Vogt, D.; Hejduk, T. Relationships between Insufficient Drinking Water Supply and the Socio-Economic Development of Small Municipalities: Mayors' Opinions from the Czech Republic. *Water* **2021**, *13*, 2098. [CrossRef]
29. Carter, J.G.; Cavan, G.; Connelly, A.; Guy, S.; Handley, J.; Kazmierczak, A. Climate change and the city: Building capacity for urban adaptation. *Prog. Plann.* **2015**, *95*, 1–66. [CrossRef]
30. Castán Broto, V.; Robin, E. Climate urbanism as critical urban theory. *Urban Geogr.* **2021**, *42*, 715–720. [CrossRef]
31. Wamsler, C.; Brink, E. Planning for climatic extremes and variability: A review of Swedish municipalities' adaptation responses. *Sustainability* **2014**, *6*, 1359–1385. [CrossRef]
32. Nyayapathi, P.; Santosh Basina, S.; Penki, R.; Basina, S.S. An Integrated GIS-AHP based Drought vulnerability Assessment for Kurnool district, Andhra Pradesh, India. *Ecocycles* **2022**, *9*, 32–48. [CrossRef]
33. Alharbi, R.S.; Nath, S.; Faizan, O.M.; Hasan, M.S.U.; Alam, S.; Khan, M.A.; Bakshi, S.; Sahana, M.; Saif, M.M. Assessment of Drought vulnerability through an integrated approach using AHP and Geoinformatics in the Kangsabati River Basin. *J. King Saud Univ.–Sci.* **2022**, *34*, 102332. [CrossRef]
34. Park, H.; Kim, K.; Lee, D.K. Prediction of severe drought area based on random forest: Using satellite image and topography data. *Water* **2019**, *11*, 705. [CrossRef]

35. Rouse, J.W.J.; Haas, R.H.; Schelll, J.A.; Deering, D.W. Monitoring vegetation systems in the great plains with erts. In Proceedings of the Oddard Space Flight Center 3d ERTS-1 Symp, Washington, DC, USA, 10–14 December 1973; Volume 1, pp. 48–62.
36. Dong, H.; Li, J.; Yuan, Y.; You, L.; Chen, C. A component-based system for agricultural drought monitoring by remote sensing. *PLoS ONE* **2017**, *12*, e0188687. [CrossRef]
37. Goetz, S.J. Multi-sensor analysis of NDVI, surface temperature and biophysical variables at a mixed grassland site. *Int. J. Remote Sens.* **1997**, *18*, 71–94. [CrossRef]
38. Liang, S.; Liu, T.; Chen, Z.; Sui, X.; Hou, X.; Wang, M.; Yao, H. *Remote Sensing Monitoring of Drought Based on Landsat8 and NDVI-Ts Characteristic Space Method*; Springer International Publishing: Berlin/Heidelberg, Germany, 2019; Volume 545, ISBN 9783030061364.
39. Lamchin, M.; Lee, W.K.; Jeon, S.W.; Lee, J.Y.; Song, C.; Piao, D.; Lim, C.H.; Khaulenbek, A.; Navaandorj, I. Correlation between desertification and environmental variables using remote sensing techniques in Hogno Khaan, Mongolia. *Sustainability* **2017**, *9*, 581. [CrossRef]
40. Ma, Z.; Shi, Z.; Zhou, Y.; Xu, J.; Yu, W.; Yang, Y. A spatial data mining algorithm for downscaling TMPA 3B43 V7 data over the Qinghai–Tibet Plateau with the effects of systematic anomalies removed. *Remote Sens. Environ.* **2017**, *200*, 378–395. [CrossRef]
41. Ihinegbu, C.; Ogunwumi, T. Multi-criteria modelling of drought: A study of Brandenburg Federal State, Germany. *Model. Earth Syst. Environ.* **2022**, *8*, 2035–2049. [CrossRef]
42. Zahradníček, P.; Brázdil, R.; Řehoř, J.; Lhotka, O.; Dobrovolný, P.; Štěpánek, P.; Trnka, M. Temperature extremes and circulation types in the Czech Republic, 1961–2020. *Int. J. Climatol.* **2022**, *42*, 4808–4829. [CrossRef]
43. Laaha, G.; Gauster, T.; Tallaksen, L.M.; Vidal, J.P.; Stahl, K.; Prudhomme, C.; Heudorfer, B.; Vlnas, R.; Ionita, M.; Van Lanen, H.A.J.; et al. The European 2015 drought from a hydrological perspective. *Hydrol. Earth Syst. Sci.* **2017**, *21*, 3001–3024. [CrossRef]
44. Dębiec, K. Drought in the Czech Republic the Political, Economic and Social Consequences. Strzelczyk, T., Ed.; Centre for Eastern Studies: Warszawa, Poland, 2021; ISBN 978-83-65827-92-0.
45. Dubrovsky, M.; Trnka, M.; Holman, I.P.; Svobodova, E.; Harrison, P.A. Developing a reduced-form ensemble of climate change scenarios for Europe and its application to selected impact indicators. *Clim. Chang.* **2015**, *128*, 169–186. [CrossRef]
46. Čermák, P.; Mikita, T.; Kadavý, J.; Trnka, M. Evaluating recent and future climatic suitability for the cultivation of norway spruce in the czech republic in comparison with observed tree cover loss between 2001 and 2020. *Forests* **2021**, *12*, 1687. [CrossRef]
47. Ho, T.K. Random decision forests. *Proc. Int. Conf. Doc. Anal. Recognit. ICDAR* **1995**, *1*, 278–282. [CrossRef]
48. Breiman, L. Bagging predictors. *Mach. Learn.* **1996**, *24*, 123–140. [CrossRef]
49. Breiman, L. Random Forests. *Mach. Learn.* **2001**, *45*, 5–32. [CrossRef]
50. Tyralis, H.; Papacharalampous, G.; Langousis, A. A brief review of random forests for water scientists and practitioners and their recent history in water resources. *Water* **2019**, *11*, 910. [CrossRef]
51. Probst, P.; Wright, M.N.; Boulesteix, A.L. Hyperparameters and tuning strategies for random forest. *Wiley Interdiscip. Rev. Data Min. Knowl. Discov.* **2019**, *9*, e1301. [CrossRef]
52. Zanon, B.; Verones, S. Climate change, urban energy and planning practices: Italian experiences of innovation in land management tools. *Land Use Policy* **2013**, *32*, 343–355. [CrossRef]
53. Ren, C.; Lau, K.L.; Yiu, K.P.; Ng, E. The application of urban climatic mapping to the urban planning of high-density cities: The case of Kaohsiung, Taiwan. *Cities* **2013**, *31*, 1–16. [CrossRef]
54. Glaas, E.; Hjerpe, M.; Storbjörk, S.; Neset, T.S.; Bohman, A.; Muthumanickam, P.; Johansson, J. Developing transformative capacity through systematic assessments and visualization of urban climate transitions. *Ambio* **2019**, *48*, 515–528. [CrossRef] [PubMed]
55. Olson, J.M. Spectrally Encoded Two-Variable Maps on JSTOR. *Ann. Assoc. Am. Geogr.* **1981**, *71*, 259–276. [CrossRef]
56. Lucchesi, L.R.; Wikle, C.K. Visualizing uncertainty in areal data with bivariate choropleth maps, map pixelation and glyph rotation. *Stat* **2017**, *6*, 292–302. [CrossRef]
57. Neij, L.; Heiskanen, E. Municipal climate mitigation policy and policy learning—A review. *J. Clean. Prod.* **2021**, *317*, 128348. [CrossRef]
58. Ekstrom, J.A.; Moser, S.C. Identifying and overcoming barriers in urban climate adaptation: Case study findings from the San Francisco Bay Area, California, USA. *Urban Clim.* **2014**, *9*, 54–74. [CrossRef]
59. EEA—European Environmental Agency. *Urban Adaptation in Europe: How Cities and Towns Respond to Climate Change*; European Environmental Agency: Copenhagen, Denmark, 2020; ISBN 9789294802705.
60. Ricciardi, G.; Ellena, M.; Barbato, G.; Giugliano, G.; Schiano, P.; Leporati, S.; Traina, C.; Mercogliano, P. Climate change adaptation cycle for pilot projects development in small municipalities: The northwestern Italian regions case study. *City Environ. Interact.* **2023**, *17*, 100097. [CrossRef]
61. Miller, E.; Buys, L. The Impact of Social Capital on Residential Water-Affecting Behaviors in a Drought-Prone Australian Community. *Soc. Nat. Resour.* **2008**, *21*, 244–257. [CrossRef]
62. Ray Biswas, R.; Rahman, A. Adaptation to climate change: A study on regional climate change adaptation policy and practice framework. *J. Environ. Manag.* **2023**, *336*, 117666. [CrossRef] [PubMed]
63. Lioubimtseva, E.; da Cunha, C. Local climate change adaptation plans in the US and France: Comparison and lessons learned in 2007–2017. *Urban Clim.* **2020**, *31*, 100577. [CrossRef]

64. Konečný, O.; Šerý, O.; Kozumplíková, A.; Stanojević, M.; Trojan, J.; Lehejček, J. Vlasnictví zemědělské půdy: Rozvojový stimul, dědictví . . . Prostředek snížení negativních dopadů klimatické změny? In Proceedings of the 25th International Colloquium on Regional Sciences, Brno, Czech Republic, 22–24 June 2022; Klímová, V., Žítek, V., Eds.; Masaryk University: Brno, Czech Republic, 2022; pp. 408–417.
65. Boulesteix, A.L.; Janitza, S.; Kruppa, J.; König, I.R. Overview of random forest methodology and practical guidance with emphasis on computational biology and bioinformatics. *Wiley Interdiscip. Rev. Data Min. Knowl. Discov.* **2012**, *2*, 493–507. [CrossRef]
66. Díaz-Uriarte, R.; Alvarez de Andrés, S. Gene selection and classification of microarray data using random forest. *BMC Bioinform.* **2006**, *7*, 3. [CrossRef]
67. Ziegler, A.; König, I.R. Mining data with random forests: Current options for real-world applications. *Wiley Interdiscip. Rev. Data Min. Knowl. Discov.* **2014**, *4*, 55–63. [CrossRef]
68. Hengl, T.; Nussbaum, M.; Wright, M.N.; Heuvelink, G.B.M.; Gräler, B. Random forest as a generic framework for predictive modeling of spatial and spatio-temporal variables. *PeerJ* **2018**, *6*, e5518. [CrossRef]
69. Schubach, M.; Re, M.; Robinson, P.N.; Valentini, G. Imbalance-Aware Machine Learning for Predicting Rare and Common Disease-Associated Non-Coding Variants. *Sci. Rep.* **2017**, *7*, 2959. [CrossRef]
70. Čermák, P.; Mikita, T.; Trnka, M.; Štěpáneke, P.; Jurečka, F.; Kusbach, A.; Šebesta, J.A.N. Changes in climate characteristics of forest altitudinal zones within the Czech Republic and their possible consequences for forest species composition. *Balt. For.* **2018**, *24*, 234–248.
71. Suggitt, A.J.; Wilson, R.J.; Isaac, N.J.B.; Beale, C.M.; Auffret, A.G.; August, T.; Bennie, J.J.; Crick, H.Q.P.; Duffield, S.; Fox, R.; et al. Extinction risk from climate change is reduced by microclimatic buffering. *Nat. Clim. Chang.* **2018**, *8*, 713–717. [CrossRef]
72. Castelli, G.; Castelli, F.; Bresci, E. Mesoclimate regulation induced by landscape restoration and water harvesting in agroecosystems of the horn of Africa. *Agric. Ecosyst. Environ.* **2019**, *275*, 54–64. [CrossRef]
73. Zhang, F.; Chen, Y.; Wang, W.; Jim, C.Y.; Zhang, Z.; Tan, M.L.; Liu, C.; Chan, N.W.; Wang, D.; Wang, Z.; et al. Impact of land-use/land-cover and landscape pattern on seasonal in-stream water quality in small watersheds. *J. Clean. Prod.* **2022**, *357*, 131907. [CrossRef]
74. Salathé, E.P.; Leung, L.R.; Qian, Y.; Zhang, Y. Regional climate model projections for the State of Washington. *Clim. Chang.* **2010**, *102*, 51–75. [CrossRef]
75. Trnka, M.; Dubrovský, M.; Žalud, Z. Climate change impacts and adaptation strategies in spring barley production in the Czech Republic. *Clim. Chang.* **2004**, *64*, 227–255. [CrossRef]
76. Schwantes, A.M.; Parolari, A.J.; Swenson, J.J.; Johnson, D.M.; Domec, J.C.; Jackson, R.B.; Pelak, N.; Porporato, A. Accounting for landscape heterogeneity improves spatial predictions of tree vulnerability to drought. *New Phytol.* **2018**, *220*, 132–146. [CrossRef]
77. Mina, M.; Messier, C.; Duveneck, M.J.; Fortin, M.J.; Aquilué, N. Managing for the unexpected: Building resilient forest landscapes to cope with global change. *Glob. Chang. Biol.* **2022**, *28*, 4323–4341. [CrossRef]
78. Homsi, R.; Shiru, M.S.; Shahid, S.; Ismail, T.; Harun, S.B.; Al-Ansari, N.; Chau, K.W.; Yaseen, Z.M. Precipitation projection using a CMIP5 GCM ensemble model: A regional investigation of Syria. *Eng. Appl. Comput. Fluid Mech.* **2020**, *14*, 90–106. [CrossRef]
79. Blažka, P.; Fischer, Z. Moisture, Water Holding, Drying and Wetting in Forest Soils. *Open J. Soil Sci.* **2014**, *04*, 174–184. [CrossRef]
80. Boeing, F.; Rakovec, O.; Kumar, R.; Samaniego, L.; Schrön, M.; Hildebrandt, A.; Rebmann, C.; Thober, S.; Müller, S.; Zacharias, S.; et al. High-resolution drought simulations and comparison to soil moisture observations in Germany. *Hydrol. Earth Syst. Sci.* **2022**, *26*, 5137–5161. [CrossRef]